ACS Energy LETTERS

http://pubs.acs.org/journal/aelccp

Plasma Catalyst-Integrated System for Ammonia Production from H_2O and N_2 at Atmospheric Pressure

Iqbal Muzammil,[#] You-Na Kim,[#] Hongjae Kang, Duy Khoe Dinh, Seongil Choi, Chanmi Jung, Young-Hoon Song, Eunseok Kim, Ji Man Kim, and Dae Hoon Lee*

Cite This: *ACS Energy Lett.* 2021, 6, 3004−3010

Read Online

ACCESS | Metrics & More | Article Recommendations | Supporting Information

ABSTRACT: **Plasma technology is considered a sustainable and clean technology for the conversion of naturally abundant compounds (i.e., water (H_2O) and nitrogen gas (N_2)) into energy-abundant compounds (e.g., hydrogen gas (H_2), ammonia (NH_3)) or chemical feed molecules (e.g., nitric oxide (NO)). Here, we report a plasma catalyst-integrated system for sustainable ammonia production, which can facilitate massive, localized ammonia production. This study demonstrates the single-step cogeneration of H_2 and nitric oxides (NO_x) from H_2O in the nitrogen discharge used for ammonia production, which proceeded via the catalytic reduction of NO_x by H_2. The proposed plasma technique yields higher NO and H_2 concentrations than conventional plasma methods, which were used to obtain an ammonia concentration of ∼0.84% with a selectivity of ∼95% and a production rate of 120 μmol/s. These promising results provide a breakthrough in the transition toward sustainable and environmentally friendly ammonia production.**

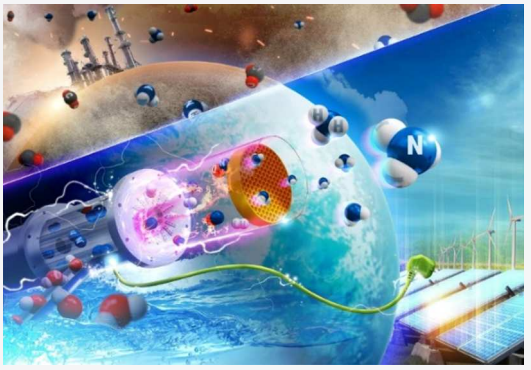

Increasing fossil-free global energy demands have motivated the scientific community to investigate new, clean, and sustainable techniques that can meet such demands. The production of clean and sustainable fuel and energy storage materials, such as ammonia (NH_3), from base molecules (i.e., water (H_2O) and nitrogen gas (N_2)) using electricity from renewable sources shows substantial potential to solve energy issues in an environmentally friendly manner.[1−3] However, the global annual NH_3 production is 150 million tons and is dominated by the Haber−Bosch process (which has a significant carbon footprint) through the following reaction (eq 1):[4]

$$N_2 + 3H_2 \leftrightarrow 2NH_3 \quad (1)$$

The synthesis of NH_3 from N_2 and hydrogen gas (H_2) is thermodynamically favored ($\Delta H^\circ_{298\ K} = -45.9$ kJ/mol). Despite continuous improvements and an efficiency close to the theoretical thermal efficiency, the Haber−Bosch process, which normally operates under high temperatures (350−550 °C) and pressures (15−35 MPa),[5] requires large amounts of energy. This is because of the high kinetic barrier for the activation of N_2 and its conversion to NH_3.[6] In addition to the large energy requirement, this reaction is responsible for 1.6% of the annual global carbon dioxide (CO_2) emissions because it uses natural gas to obtain H_2 and energy. Moreover, the Haber−Bosch process is not appropriate for decentralized production, which utilizes renewable energy with intermittency, owing to the temperature and pressure conditions required for this process (Figure 1a).[7,8]

As alternatives to the Haber−Bosch process, various catalysts have been investigated by electrochemical methods for NH_3 synthesis under mild conditions (ambient temperature and pressure). The synthesis of NH_3 through a nitrogen reduction reaction (NRR) using H_2 and a catalyst exhibits slow reaction kinetics due to the chemical inertness of N_2 molecules. Ruthenium-based catalysts have been extensively examined owing to their high activity at low temperatures (100−150 °C). The production of NH_3 by electrochemical NRR using renewable electricity is a potential solution to reduce the CO_2 emissions of the NH_3 production process.

Received: July 19, 2021
Accepted: August 4, 2021

https://doi.org/10.1021/acsenergylett.1c01497
ACS Energy Lett. 2021, 6, 3004−3010

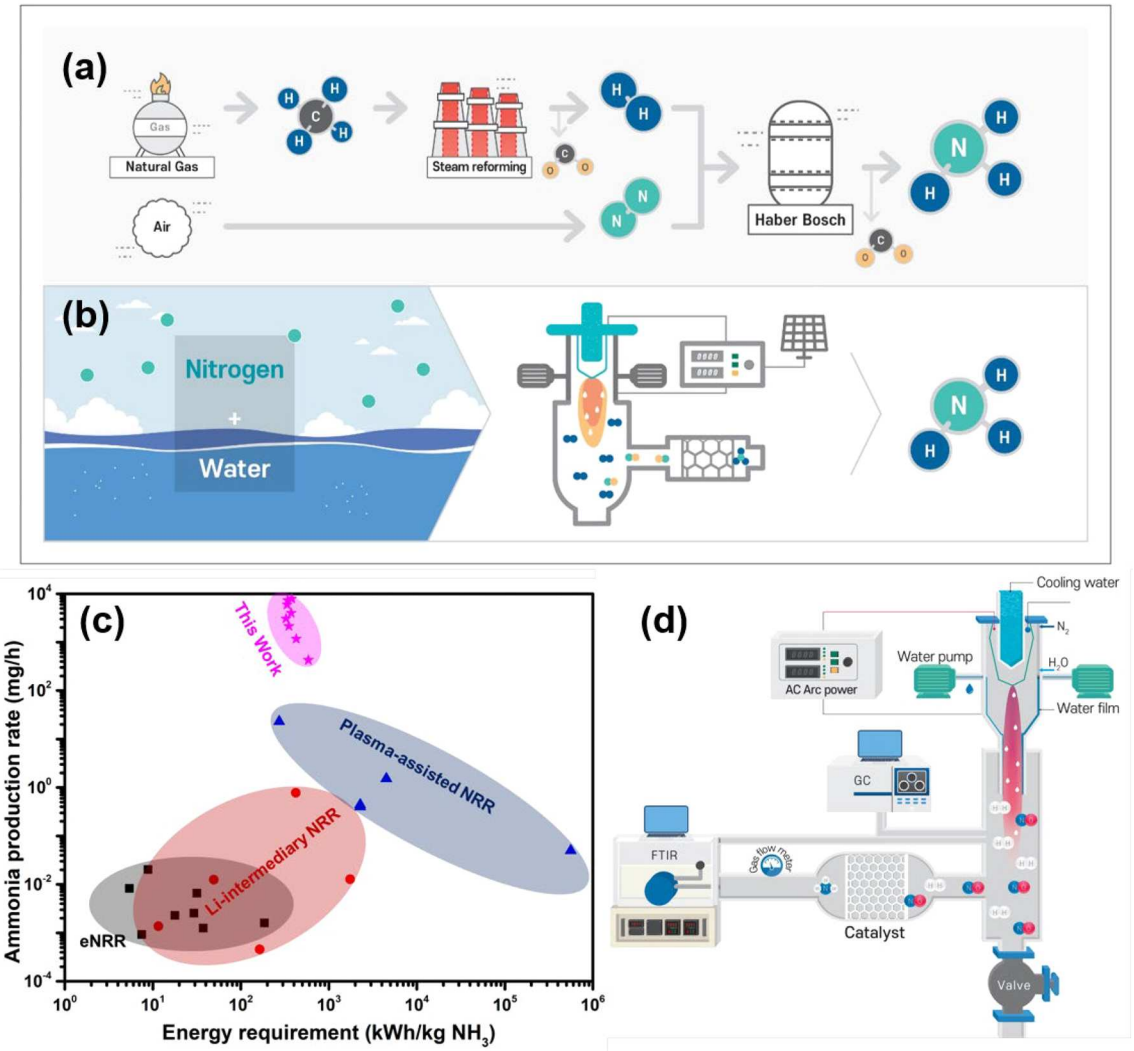

Figure 1. Schematics illustrating the (a) Haber–Bosch process and (b) the proposed novel plasma catalyst-integrated system for ammonia (NH_3) synthesis. Here, rotating gliding arc (RGA) plasma is used to produce hydrogen gas (H_2) and nitric oxide (NO) from water (H_2O) and nitrogen gas (N_2); NO is reduced by H_2 to form NH_3 via catalytic reduction. (c) NH_3 production rate and energy consumption compared with recently reported state-of-the-art results: pink stars, this study; black squares, direct electrocatalytic nitrogen reduction reaction (eNRR); red circles, Li-intermediary NRR; and blue triangles, plasma-assisted NRR.[9] Table S3 (Supporting Information) provides detailed data. (d) Schematic of the proposed plasma catalyst-integrated system for highly selective NH_3 production with Fourier-transform infrared spectroscopy (FTIR).

Several groups have reported electrochemical NH_3 synthesis from H_2O and air with Faradaic efficiencies of ~60%.[10,11] Recently, the electrocatalytic NRR (eNRR) for NH_3 production under mild conditions has been investigated; however, this process exhibits limited activity and a low NH_3 production rate (Figure 1c).[12−18] The Li redox intermediary NRR (Li-NRR) has overcome the limitations of eNRR by converting N_2 into a more reactive intermediary form. However, this process requires a significant minimum overpotential of 3 V, ultradry and oxygen-free organic solvents, high pressures (~50 bar), pure hydrogen and nitrogen feedstocks, and Li metal (Figure 1c).[19−24]

NRRs for NH_3 production from plasma–liquid interactions have been recently reported; and although these studies are promising for reducing fossil fuel dependence, their NH_3 production rates are low (Figure 1c and Table S3, Supporting Information).[1,9,25−31] Further efforts to improve such integrated systems are necessary to enhance NH_3 production.

Nitric oxides (NO_x) are more easily reduced to NH_3 by hydrogen in the presence of noble metal catalysts (e.g., those containing Pt, Pd, Ru, and Os) than N_2.[32] Despite the large number of studies on plasma nitrogen fixation published in the last 30 years, there are no studies on the oxygen-free cogeneration of H_2 and NO, which are valuable chemical feedstocks for NH_3 production; however, they are generally produced separately in multiple steps.[33−37] Several previous reports mention the cogeneration of other nitrogen species (NO, NO_2, and HNO_3), whose concentrations are on the scale of several hundred ppm.[38−40] While these concentrations are too low to be considered useful for nitrogen fixation, they will still yield several environmental problems.[41] A solid-oxide electrolysis cell combined with a radiofrequency plasma source was recently used for the cogeneration of NO_x and H; however, this hybrid technique produced a low NO_x (0.08%) concentration.[42]

In this study, we developed a novel, continuous, scalable, and single-step plasma-catalyst integrated technology for NH_3

https://doi.org/10.1021/acsenergylett.1c01497
ACS Energy Lett. 2021, 6, 3004−3010

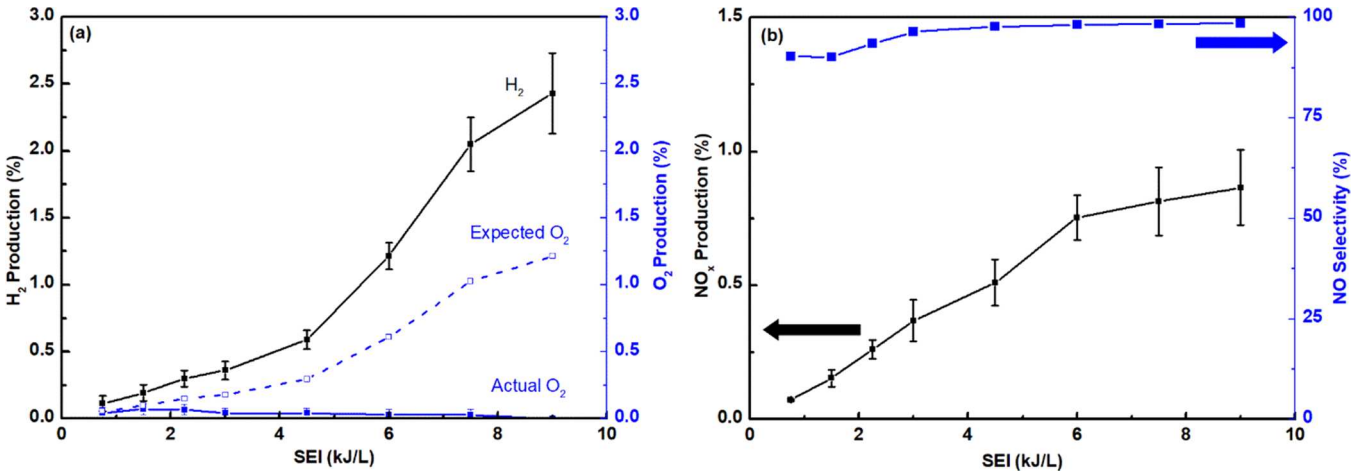

Figure 2. (a) H_2 and oxygen gas (O_2) production and (b) the production of nitric oxides (NO_x; NO + NO_2) and NO selectivity as functions of the specific energy input (SEI). Error bars for H_2 and O_2 are based on gas chromatography measurements of three independent experiments. Error bars for NO_x are based on continuous, 10 min measurements with a 5 s FTIR scan interval.

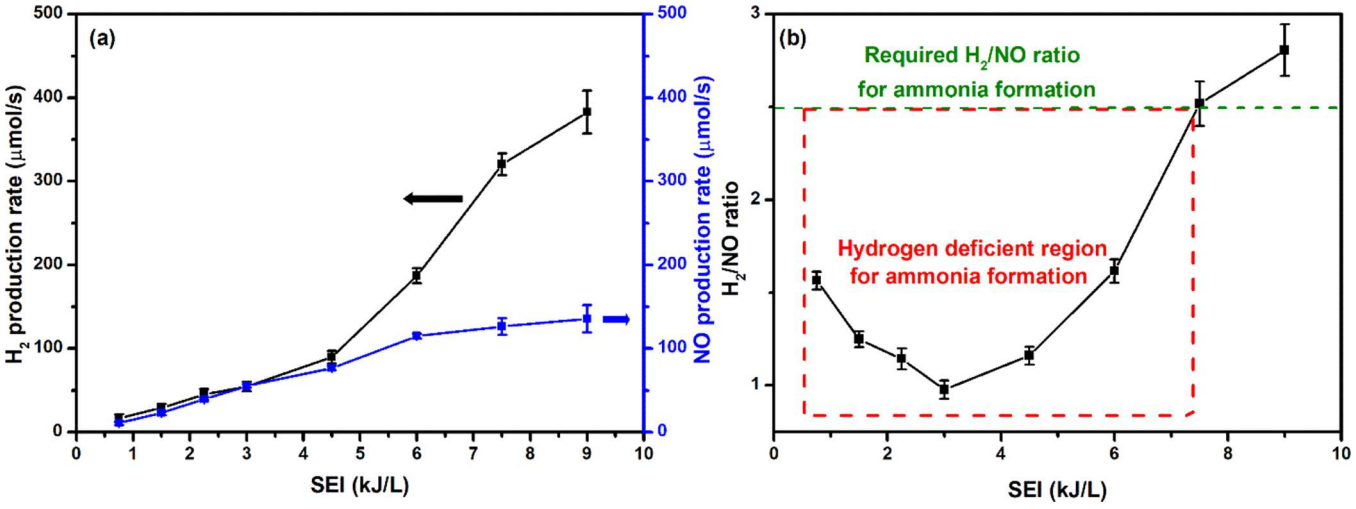

Figure 3. (a) H_2 and NO_x formation rates and (b) H_2/NO ratios for NH_3 formation as a function of the SEI. Error bars for H_2 and O_2 are based on gas chromatography measurements of three independent experiments. Error bars for NO_x are based on continuous, 10 min measurements with a 5 s FTIR scan interval.

generation via a H_2 and NO intermediary approach. Our approach is based on the coupling of two technologies: (I) H_2O splitting in the nitrogen discharge using a rotating gliding arc (RGA) to produce H_2 and NO; (II) intermediary NO reduced via H_2 to produce NH_3 in the presence of noble-metal catalysts. N_2 was tangentially fed at a rate of at 20 L/min into the reactor through two holes at the bottom of the cylindrical ground to provide a swirling flow to rotate the arc. In this unique system, liquid water was introduced in the form of a water film at a rate of 50 mL/min into the nitrogen discharge from exactly the center of the surrounding wall of the reactor; this form was used to assist in reactor cooling and not destabilize the arc. The arc discharge was driven by an AC power source with a high-voltage transformer that can supply up to 6 kV and a current of up to 20 A at a frequency of 20 kHz. The highly energetic electrons and active nitrogen species collided with the water film and ionized/dissociated into H and OH/O radicals. The OH/O radicals further reacted with the nitrogen radicals to form NO_x. The generated NO and H_2 were injected into the Pd/γ-Al_2O_3 catalyst on a ceramic monolith connected to the plasma reactor. Previous studies have reported that Pd catalysts are the most active for NO reduction via H_2 to produce NH_3.[43] The Pd catalyst was directly heated by injected hot gas (and therefore did not require an external heating source); the temperature was controlled in the range of 100−110 °C by changing the flow rate of the catalyst system. As plasma heating is rapid, it does not require an extended period to reach the required catalyst light-off temperature. The NO_x was completely reduced by the cogenerated H_2 to produce NH_3 with a 95% selectivity. The Supporting Information provides further details on the experimental setup and optimized conditions.

Figure 2 shows the H_2, O_2, and NO_x production rates (%) during water splitting in the nitrogen discharge as a function of the specific energy input (SEI). The SEI was varied by changing discharge power with a constant N_2 flow of 20 L/min. The continuous increase in the SEI increased the H_2 production rate, which confirmed that no secondary reactions with hydrogen occurred during plasma H_2O splitting, as shown in Figure 2a. In addition to H_2, O_2 also formed during H_2O splitting and followed the trend of stoichiometric H_2O splitting at a low SIE (0.75 kJ/L); however, the O_2 production rate

https://doi.org/10.1021/acsenergylett.1c01497
ACS Energy Lett. 2021, 6, 3004−3010

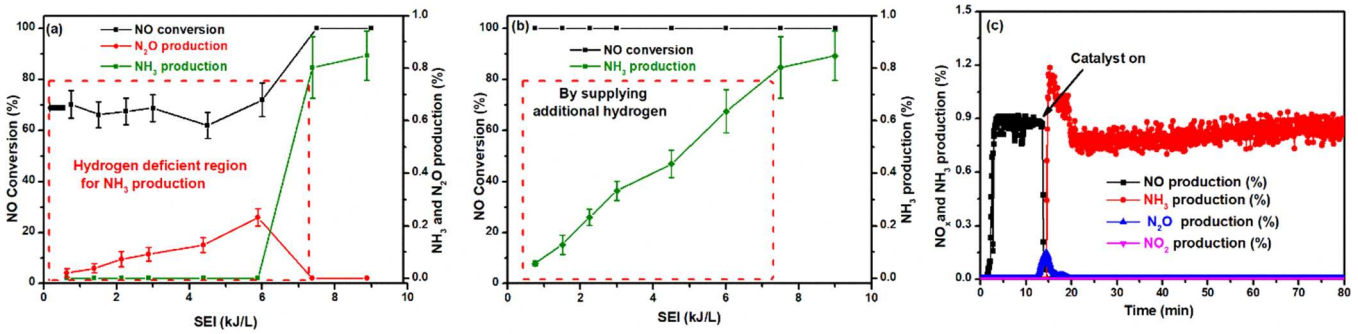

Figure 4. NO_x conversion and resultant products: (a) without a supply of additional H_2 and (b) by supplying additional H_2 in the H_2 deficient region as a function of SEI. (c) NO_x and NH_3 production at ∼9 kJ/L as functions of time based on continuous measurements with a 5 s FTIR scan interval. Error bars for H_2 and O_2 are based on gas chromatography measurements of three independent experiments. Error bars for NO_x and NH_3 are based on continuous, 10 min measurements with a 5 s FTIR scan interval.

began to decrease as the SEI was further increased until it was ultimately completely removed. The disappearance of O_2 with a high SEI indicates the presence of secondary reactions involving O and N atoms. This assumption was confirmed by Fourier transform infrared spectroscopy (FTIR) and a commercially available NO_x-emissions monitoring system (MRU air fair) based on infrared and electrochemical sensors. The presence of NO_x (NO + NO_2) was observed in the FTIR spectra (Figure S2 in the Supporting Information). Figure 2b shows that at a low SEI, NO_x production was limited (0.07%) and continuously increased with an increase in the SEI. The NO_x production at an SEI of 3 kJ/L was 0.37%, which is approximately equivalent to the H_2 production (0.4%). The almost identical H_2 and NO_x production rates confirmed the disappearance of O_2, satisfying the stoichiometric equation for H_2O splitting. However, further increase in the SEI from 3 to 9 kJ/L showed sigmoidal growth in H_2 and NO_x production from ∼0.4% to ∼2.4% and ∼0.37% to ∼0.9%, respectively. These nonlinear increases in the H_2 and NO_x production rates again resulted in out-of-equilibrium stoichiometric H_2O splitting in the nitrogen discharge, which can be explained by metallic particles produced as a result of reactor erosion at a high SEI. Metallic particles serve as supporting materials for the H_2 evolution reaction, which forms metallic oxides and H_2[44,45] (see Supporting Information).

In Figure 3a, the H_2 and NO production rates are displayed according to the SEI. The H_2 and NO formation rates increased in the same manner as the production rates until an SEI of 3 kJ/L was reached; however, further increase in the SEI resulted in a substantial increase in the H_2 formation rate and a slight increase in the NO formation rate (Figure 3a). This unusual change in the H_2/NO ratio was beneficial for NH_3 production, as shown in Figure 3b. The H_2/NO ratio was 1.5 for the reaction at 0.75 kJ/L because the NO formation rate was low and the H_2 formation rate was high, which resulted in insufficient H_2 to synthesize NH_3. Further increase in the SEI from 0.75 to 3 kJ/L decreased the H_2/NO ratio to 1, as more O was available for NO formation. Increasing the SEI further also enhanced the H_2/NO ratio; at 7.5 kJ/L, the SEI attained a sufficient H_2/NO ratio (∼2.5) for NH_3 formation. Figure 3b shows the H_2 deficient and sufficient regions for NH_3 formation.

As noted above, we demonstrated that H_2 and NO can be generated by H_2O splitting with a differential H_2/NO ratio; these are essential feeds for NH_3 production. To investigate the catalytic reduction of NO, the catalyst was connected to the outlet of the plasma reactor (Figure 1). Catalytic reduction was carried out at ∼110 °C, and the reaction temperature was maintained by the heat generated from the plasma reaction that was tuned by controlling the pipe length and flow rate. Figure 4a shows the NO conversion and concentrations of N_2O (i.e., a byproduct) and NH_3 as functions of the SEI. In the low SEI region (<7.5 kJ/L), NO conversion was <80% and N_2O and N_2 were the only products; thus, NH_3 production did not occur (see eqs 2 and 3). In this region, further increase in the SEI also increased N_2O production. At an SEI ≤ 7.5 kJ/L, the NO-to-N_2O conversion sharply decreased to 0 and the generated NO from the plasma was completely converted to NH_3 with an almost 95% selectivity for NH_3. The difference in the product selectivity according to the SEI was a result of the different H_2/NO ratios. Figure 3b shows the change in the H_2/NO ratio due to the SEI conditions; an SEI of 7.5 kJ/L was the minimum amount that provided an ideal H_2/NO ratio for NH_3 synthesis.

To confirm the effect of the H_2/NO ratio on NH_3 selectivity in our reactor system, experiments on NH_3 synthesis were repeated under the same conditions as those shown in Figure 4a, except for the injection of additional H_2 to compensate the H_2/NO ratio at 2.5 under an SEI of <7.5 kJ/L. As shown in Figure 4b, the supply of sufficient H_2, as compared with the supply of sufficient NO, not only reduced the N_2O production to 0 but also improved the NH_3 production. The results show that the NH_3 concentration was linear with an increase in the SEI. According to earlier studies, different types of products can be produced during the NO reduction reaction depending on the ratio of the reactants (eqs 2–4).[46] In this study, the production of N_2O with a limited supply of H_2 (eq 3), and the production of NH_3 with an excessive H_2 supply (eq 4) confirms that the H_2/NO ratio plays a critical role in NH_3 production via NO reduction.

$$2NO + 2H_2 \rightarrow N_2 + 2H_2O \quad (2)$$

$$2NO + H_2 \rightarrow N_2O + H_2O \quad (3)$$

$$2NO + 5H_2 \rightarrow 2NH_3 + 2H_2O \quad (4)$$

Figure 4c shows the FTIR results for NO, NO_2, N_2O, and NH_3 production with and without catalyst at an SEI of ∼9 kJ/L. For the first 12 min, NO_x was checked via FTIR by bypassing the catalyst, and then gases were allowed to pass through the catalyst that decreased the NO, and a minor amount of N_2O appeared at the start and dropped to zero quickly. Then, NH_3 production began. The production of a

https://doi.org/10.1021/acsenergylett.1c01497
ACS Energy Lett. 2021, 6, 3004−3010

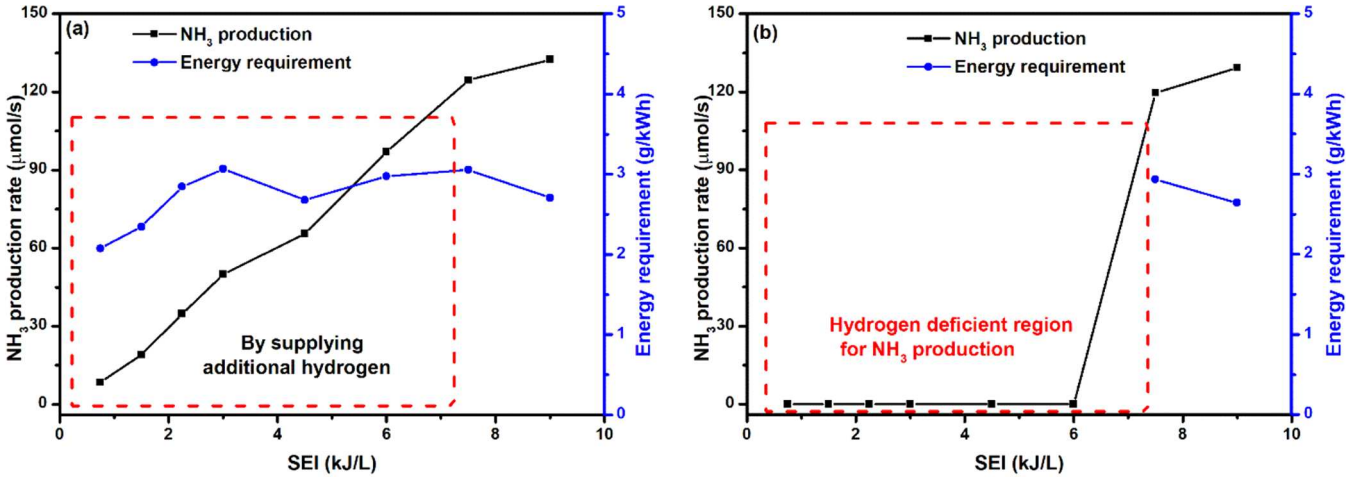

Figure 5. NH_3 production rate and energy requirements (a) upon supplying additional H_2 in the H_2 deficient region and (b) without supplying additional H_2 as functions of SEI.

small amount of N_2O right before the start of NH_3 synthesis using a catalyst is due to the initial oxidative state of Pd in the fresh catalyst. The production of NH_3 continuously increased after the reduction of the Pd catalyst by the H_2 feed.

Figure 5 shows that the rate of NH_3 production was 120 μmol/s (7348 mg/h) without the injection of additional H_2 from outside the reactor system. Compared with previous studies on NH_3 synthesis from N_2, the remarkable NH_3 yield (300−400-fold higher) and selectivity of the present work are a result of cogenerated NO and H_2 and the use of a high H_2/NO ratio in the feed.[32] The energy requirement for NH_3 production at a high SEI was 340 kWh/kg NH_3; although this energy consumption is higher than those previously reported for plasma NH_3 production, the latter only includes the cost for nitrogen fixation, not that for both nitrogen and H_2.[47] The utilization of thermal energy waste to heat the gas and water could be evaluated in future studies; we utilized this waste to heat only the catalyst. In addition to NH_3 production, the remaining H_2O after the plasma reaction contains nitrate (NO_3^-) and nitrite (NO_2^-) produced from an NO_x interacting with the water in the reactor. Water with NO_3^- and NO_2^-, which is known as plasma-activated water, is an effective plant fertilizer[48,49] (see Supporting Information). The production of plasma-activated water does not require any additional energy, and it is considered a favorable byproduct of NH_3 production. Moreover, the long-term stability of the system was verified with a 1 h continuous operation at an SEI of 7.5 kJ/L. Continuous NH_3 production without melting or degrading the reactor body revealed the significant roles of H_2O in this process; it provides H_2 and NO_x and also cools the reactor body. In the pure nitrogen discharge without the water supply (7.5 kJ/L SEI), the downstream temperature of the reactor body reached 1000 °C and the reactor began to melt. The presence of a water film in the proposed system provided a shield for the reactor body, thus lowering the outgas temperature to approximately 400 °C.

In summary, a novel plasma catalyst-integrated strategy was developed for the production of significant amounts of NH_3 from N_2 and H_2O using renewable electricity at ambient pressures. By design, this plasma/catalyst-integrated strategy is capable of an exceptionally high NH_3 production yield with high selectivity, as compared to those of other typical plasma catalyst approaches. This is due to its ability to cogenerate NO and H_2 as an NH_3 feedstock while producing sufficient heat to maintain the catalyst temperature of the NO reduction reaction, thus producing large amounts of NH_3. The demonstrated process exhibited a 95% NH_3 selectivity with a 120 μmol/s (7348 mg/h) NH_3 production rate, which is 300−400 times higher than those previously reported for plasma and electrochemical technologies. This technology also has the potential to scale up the NH_3 production rate by increasing the gas flow rate and SEI. The remaining water after plasma discharge contained NO_3^- and NO_2^-; this nitrated H_2O is an effective plant fertilizer. Only a single power source was used in the entire process for catalyst heating, raw material (NO and H_2) production, and final product (NH_3 and nitrated H_2O) generation. Although we developed a novel plasma catalyst-integrated strategy for the production of large amounts of NH_3, continuous research in this area, especially regarding the control of the H_2/NO ratio to obtain optimal conditions for catalytic NO reduction, could eventually lead to the replacement of the classic Haber−Bosch process. The initial production and cost analyses of the proposed system are promising for achieving the long-term goal of energy and environmental sustainability as they pertain to NH_3 production.

■ ASSOCIATED CONTENT

Supporting Information

The Supporting Information is available free of charge at https://pubs.acs.org/doi/10.1021/acsenergylett.1c01497.

S.1 Experimental details, S.2 Optimized conditions for the cogeneration of nitric oxide and hydrogen, S.3 Reaction mechanism, S.4 Erosion process and missing oxygen, S.5 Performance benchmarking, Figures S1 to S10, and Tables S1 to S3 (PDF)

■ AUTHOR INFORMATION

Corresponding Author

Dae Hoon Lee − *Department of Plasma Engineering, Korea Institute of Machinery and Materials, Daejeon 305-343, South Korea*; Email: dhlee@kimm.re.kr

https://doi.org/10.1021/acsenergylett.1c01497
ACS Energy Lett. 2021, 6, 3004−3010

Authors

Iqbal Muzammil − *Department of Plasma Engineering, Korea Institute of Machinery and Materials, Daejeon 305-343, South Korea;* orcid.org/0000-0001-7516-9941

You-Na Kim − *Department of Plasma Engineering, Korea Institute of Machinery and Materials, Daejeon 305-343, South Korea*

Hongjae Kang − *Department of Plasma Engineering, Korea Institute of Machinery and Materials, Daejeon 305-343, South Korea*

Duy Khoe Dinh − *Department of Plasma Engineering, Korea Institute of Machinery and Materials, Daejeon 305-343, South Korea*

Seongil Choi − *Department of Plasma Engineering, Korea Institute of Machinery and Materials, Daejeon 305-343, South Korea*

Chanmi Jung − *Department of Plasma Engineering, Korea Institute of Machinery and Materials, Daejeon 305-343, South Korea*

Young-Hoon Song − *Department of Plasma Engineering, Korea Institute of Machinery and Materials, Daejeon 305-343, South Korea*

Eunseok Kim − *Heesung Catalysts Corp., Shiheung City, Kyungki-Do 429-450, South Korea; Department of Chemistry, Sungkyunkwan University, Suwon 16419, South Korea*

Ji Man Kim − *Department of Chemistry, Sungkyunkwan University, Suwon 16419, South Korea;* orcid.org/0000-0003-0860-4880

Complete contact information is available at: https://pubs.acs.org/10.1021/acsenergylett.1c01497

Author Contributions

#I.M. and Y.-N. K. are first coauthors.

Notes

The authors declare no competing financial interest.

■ ACKNOWLEDGMENTS

This study was supported by the Institutional Research Program (NK225F) and National Research Council of Science & Technology (NST) by the Korean government (MSIT) (No. CAP-18-08-KIMM).

■ REFERENCES

(1) Sharma, R. K.; Patel, H.; Mushtaq, U.; Kyriakou, V.; Zafeiropoulos, G.; Peeters, F.; Welzel, S.; van de Sanden, M. C. M.; Tsampas, M. N. Plasma Activated Electrochemical Ammonia Synthesis from Nitrogen and Water. *ACS Energy Lett.* **2021**, *6* (2), 313−319.

(2) Bogaerts, A.; Neyts, E. C. Plasma Technology: An Emerging Technology for Energy Storage. *ACS Energy Lett.* **2018**, *3* (4), 1013−1027.

(3) Swearer, D. F.; Knowles, N. R.; Everitt, H. O.; Halas, N. J. Light-Driven Chemical Looping for Ammonia Synthesis. *ACS Energy Lett.* **2019**, *4* (7), 1505−1512.

(4) Smith, C.; Hill, A. K.; Torrente-Murciano, L. Current and Future Role of Haber-Bosch Ammonia in a Carbon-Free Energy Landscape. *Energy Environ. Sci.* **2020**, *13* (2), 331−344.

(5) Smil, V. *Enriching the Earth: Fritz Haber, Carl Bosch, and the Transformation of World Food Production*; MIT press, 2004.

(6) Van Der Ham, C. J. M.; Koper, M. T. M.; Hetterscheid, D. G. H. Challenges in Reduction of Dinitrogen by Proton and Electron Transfer. *Chem. Soc. Rev.* **2014**, *43*, 5183−5191.

(7) Liu, H. Ammonia Synthesis Catalyst 100 Years: Practice, Enlightenment and Challenge. *Chin. J. Catal.* **2014**, *35* (10), 1619−1640.

(8) Winter, L. R.; Chen, J. G. N2 Fixation by Plasma-Activated Processes. *Joule* **2021**, *5* (2), 300−315.

(9) Sun, J.; Alam, D.; Daiyan, R.; Masood, H.; Zhang, T.; Zhou, R.; Cullen, P. J.; Lovell, E. C.; Jalili, A.; Rouhollah; Amal, R. A Hybrid Plasma Electrocatalytic Process for Sustainable Ammonia Production. *Energy Environ. Sci.* **2021**, *14*, 865.

(10) Wang, M.; Liu, S.; Qian, T.; Liu, J.; Zhou, J.; Ji, H.; Xiong, J.; Zhong, J.; Yan, C. Over 56.55% Faradaic Efficiency of Ambient Ammonia Synthesis Enabled by Positively Shifting the Reaction Potential. *Nat. Commun.* **2019**, *10* (1), 341.

(11) Hao, Y.-C.; Guo, Y.; Chen, L.-W.; Shu, M.; Wang, X.-Y.; Bu, T.-A.; Gao, W.-Y.; Zhang, N.; Su, X.; Feng, X.; et al. Promoting Nitrogen Electroreduction to Ammonia with Bismuth Nanocrystals and Potassium Cations in Water. *Nat. Catal.* **2019**, *2* (5), 448−456.

(12) Chen, S.; Perathoner, S.; Ampelli, C.; Mebrahtu, C.; Su, D.; Centi, G. Electrocatalytic Synthesis of Ammonia at Room Temperature and Atmospheric Pressure from Water and Nitrogen on a Carbon-Nanotube-Based Electrocatalyst. *Angew. Chem., Int. Ed.* **2017**, *56* (10), 2699−2703.

(13) Bao, D.; Zhang, Q.; Meng, F.-L.; Zhong, H.-X.; Shi, M.-M.; Zhang, Y.; Yan, J.-M.; Jiang, Q.; Zhang, X.-B. Electrochemical Reduction of N2 under Ambient Conditions for Artificial N2 Fixation and Renewable Energy Storage Using N2/NH3 Cycle. *Adv. Mater.* **2017**, *29* (3), 1604799.

(14) Kordali, V.; Kyriacou, G.; Lambrou, C. Electrochemical Synthesis of Ammonia at Atmospheric Pressure and Low Temperature in a Solid Polymer Electrolyte Cell. *Chem. Commun.* **2000**, No. 17, 1673−1674.

(15) Lan, R.; Irvine, J. T. S.; Tao, S. Synthesis of Ammonia Directly from Air and Water at Ambient Temperature and Pressure. *Sci. Rep.* **2013**, *3* (1), 1145.

(16) Suryanto, B. H. R.; Wang, D.; Azofra, L. M.; Harb, M.; Cavallo, L.; Jalili, R.; Mitchell, D. R. G.; Chatti, M.; MacFarlane, D. R. MoS2 Polymorphic Engineering Enhances Selectivity in the Electrochemical Reduction of Nitrogen to Ammonia. *ACS Energy Lett.* **2019**, *4* (2), 430−435.

(17) Zhang, L.; Ding, L.-X.; Chen, G.-F.; Yang, X.; Wang, H. Ammonia Synthesis Under Ambient Conditions: Selective Electroreduction of Dinitrogen to Ammonia on Black Phosphorus Nanosheets. *Angew. Chem., Int. Ed.* **2019**, *58* (9), 2612−2616.

(18) Wang, J.; Yu, L.; Hu, L.; Chen, G.; Xin, H.; Feng, X. Ambient Ammonia Synthesis via Palladium-Catalyzed Electrohydrogenation of Dinitrogen at Low Overpotential. *Nat. Commun.* **2018**, *9* (1), 1795.

(19) Andersen, S. Z.; Čolić, V.; Yang, S.; Schwalbe, J. A.; Nielander, A. C.; McEnaney, J. M.; Enemark-Rasmussen, K.; Baker, J. G.; Singh, A. R.; Rohr, B. A.; et al. A Rigorous Electrochemical Ammonia Synthesis Protocol with Quantitative Isotope Measurements. *Nature* **2019**, *570* (7762), 504−508.

(20) Lazouski, N.; Chung, M.; Williams, K.; Gala, M. L.; Manthiram, K. Non-Aqueous Gas Diffusion Electrodes for Rapid Ammonia Synthesis from Nitrogen and Water-Splitting-Derived Hydrogen. *Nat. Catal.* **2020**, *3* (5), 463−469.

(21) Lazouski, N.; Schiffer, Z. J.; Williams, K.; Manthiram, K. Understanding Continuous Lithium-Mediated Electrochemical Nitrogen Reduction. *Joule* **2019**, *3* (4), 1127−1139.

(22) Lee, H. K.; Koh, C. S. L.; Lee, Y. H.; Liu, C.; Phang, I. Y.; Han, X.; Tsung, C.-K.; Ling, X. Y. Favoring the Unfavored: Selective Electrochemical Nitrogen Fixation Using a Reticular Chemistry Approach. *Sci. Adv.* **2018**, *4* (3), 3208.

(23) Pappenfus, T. M.; Lee, K.; Thoma, L. M.; Dukart, C. R. Wind to Ammonia: Electrochemical Processes in Room Temperature Ionic Liquids. *ECS Trans.* **2009**, *16* (49), 89−93.

(24) Chen, G.-F.; Cao, X.; Wu, S.; Zeng, X.; Ding, L.-X.; Zhu, M.; Wang, H. Ammonia Electrosynthesis with High Selectivity under Ambient Conditions via a Li+ Incorporation Strategy. *J. Am. Chem. Soc.* **2017**, *139* (29), 9771−9774.

(25) Haruyama, T.; Namise, T.; Shimoshimizu, N.; Uemura, S.; Takatsuji, Y.; Hino, M.; Yamasaki, R.; Kamachi, T.; Kohno, M. Non-Catalyzed One-Step Synthesis of Ammonia from Atmospheric Air and Water. *Green Chem.* **2016**, *18* (16), 4536−4541.
(26) Hawtof, R.; Ghosh, S.; Guarr, E.; Xu, C.; Mohan Sankaran, R.; Renner, J. N. Catalyst-Free, Highly Selective Synthesis of Ammonia from Nitrogen and Water by a Plasma Electrolytic System. *Sci. Adv.* **2019**, *5* (1), eaat5778.
(27) Kumari, S.; Pishgar, S.; Schwarting, M. E.; Paxton, W. F.; Spurgeon, J. M. Synergistic Plasma-Assisted Electrochemical Reduction of Nitrogen to Ammonia. *Chem. Commun.* **2018**, *54* (95), 13347−13350.
(28) Gorbanev, Y.; Vervloessem, E.; Nikiforov, A.; Bogaerts, A. Nitrogen Fixation with Water Vapor by Nonequilibrium Plasma: Toward Sustainable Ammonia Production. *ACS Sustainable Chem. Eng.* **2020**, *8* (7), 2996−3004.
(29) Peng, P.; Chen, P.; Addy, M.; Cheng, Y.; Zhang, Y.; Anderson, E.; Zhou, N.; Schiappacasse, C.; Hatzenbeller, R.; Fan, L.; et al. In Situ Plasma-Assisted Atmospheric Nitrogen Fixation Using Water and Spray-Type Jet Plasma. *Chem. Commun.* **2018**, *54* (23), 2886−2889.
(30) Wang, Y.; Craven, M.; Yu, X.; Ding, J.; Bryant, P.; Huang, J.; Tu, X. Plasma-Enhanced Catalytic Synthesis of Ammonia over a Ni/Al2O3 Catalyst at Near-Room Temperature: Insights into the Importance of the Catalyst Surface on the Reaction Mechanism. *ACS Catal.* **2019**, *9* (12), 10780−10793.
(31) Lamichhane, P.; Adhikari, B. C.; Nguyen, L. N.; Paneru, R.; Ghimire, B.; Mumtaz, S.; Lim, J. S.; Hong, Y. J.; Choi, E. H. Sustainable Nitrogen Fixation from Synergistic Effect of Photo-Electrochemical Water Splitting and Atmospheric Pressure N2 Plasma. *Plasma Sources Sci. Technol.* **2020**, *29* (4), 45026.
(32) Long, J.; Chen, S.; Zhang, Y.; Guo, C.; Fu, X.; Deng, D.; Xiao, J. Direct Electrochemical Ammonia Synthesis from Nitric Oxide. *Angew. Chem., Int. Ed.* **2020**, *59* (24), 9711−9718.
(33) Shelef, M.; Gandhi, H. S. Ammonia Formation in Catalytic Reduction of Nitric Oxide by Molecular Hydrogen. II. Noble Metal Catalysts. *Ind. Eng. Chem. Prod. Res. Dev.* **1972**, *11* (4), 393−396.
(34) Shelef, M.; Gandhi, H. S. Ammonia Formation in Catalytic Reduction of Nitric Oxide by Molecular Hydrogen. I. Base Metal Oxide Catalysts. *Ind. Eng. Chem. Prod. Res. Dev.* **1972**, *11* (1), 2−11.
(35) Vanraes, P.; Bogaerts, A. Plasma Physics of Liquids - A Focused Review. *Appl. Phys. Rev.* **2018**, *5* (3), No. 031103.
(36) Bruggeman, P. J.; Kushner, M. J.; Locke, B. R.; Gardeniers, J. G. E. E.; Graham, W. G.; Graves, D. B.; Hofman-Caris, R. C. H. M. H. M.; Maric, D.; Reid, J. P.; Ceriani, E.; et al. Plasma-Liquid Interactions: A Review and Roadmap. *Plasma Sources Sci. Technol.* **2016**, *25* (5), No. 053002.
(37) Muzammil, I.; Lee, D. H.; Dinh, D. K.; Kang, H.; Roh, S. A.; Kim, Y.-N.; Choi, S.; Jung, C.; Song, Y.-H. A Novel Energy Efficient Path for Nitrogen Fixation Using a Non-Thermal Arc. *RSC Adv.* **2021**, *11* (21), 12729−12738.
(38) Porter, D.; Poplin, M. D.; Holzer, F.; Finney, W. C.; Locke, B. R. Formation of Hydrogen Peroxide, Hydrogen, and Oxygen in Gliding Arc Electrical Discharge Reactors with Water Spray. *IEEE Trans. Ind. Appl.* **2009**, *45* (2), 623−629.
(39) Burlica, R.; Shih, K.-Y.; Locke, B. R. Formation of H_2 and H_2O_2 in a Water-Spray Gliding Arc Nonthermal Plasma Reactor. *Ind. Eng. Chem. Res.* **2010**, *49* (14), 6342−6349.
(40) Zhang, H.; Zhu, F.; Li, X.; Cen, K.; Du, C.; Tu, X. Rotating Gliding Arc Assisted Water Splitting in Atmospheric Nitrogen. *Plasma Chem. Plasma Process.* **2016**, *36* (3), 813−834.
(41) Snoeckx, R.; Heijkers, S.; Van Wesenbeeck, K.; Lenaerts, S.; Bogaerts, A. CO2 Conversion in a Dielectric Barrier Discharge Plasma: N2 in the Mix as a Helping Hand or Problematic Impurity? *Energy Environ. Sci.* **2016**, *9* (3), 999−1011.
(42) Patel, H.; Sharma, R. K.; Kyriakou, V.; Pandiyan, A.; Welzel, S.; Van De Sanden, M. C. M.; Tsampas, M. N. Plasma-Activated Electrolysis for Cogeneration of Nitric Oxide and Hydrogen from Water and Nitrogen. *ACS Energy Lett.* **2019**, *4* (9), 2091−2095.
(43) Liu, Z.; Li, J.; Woo, S. I. Recent Advances in the Selective Catalytic Reduction of NOx by Hydrogen in the Presence of Oxygen. *Energy Environ. Sci.* **2012**, *5* (10), 8799−8814.
(44) Dey, G. R.; Zode, S. D.; Namboodiri, V. Application of Plasma for Efficient H 2 Production: A Realism of Copper Electrode in Single Dielectric Barrier Discharge Reactor. *Phys. Plasmas* **2018**, *25*, 103508.
(45) Deng, Y.; Handoko, A. D.; Du, Y.; Xi, S.; Yeo, B. S. In Situ Raman Spectroscopy of Copper and Copper Oxide Surfaces during Electrochemical Oxygen Evolution Reaction: Identification of CuIII Oxides as Catalytically Active Species. *ACS Catal.* **2016**, *6* (4), 2473−2481.
(46) Bai, Y.; Mavrikakis, M. Mechanistic Study of Nitric Oxide Reduction by Hydrogen on Pt(100) (I): A DFT Analysis of the Reaction Network. *J. Phys. Chem. B* **2018**, *122* (2), 432−443.
(47) Rouwenhorst, K. H. R.; Engelmann, Y.; van't Veer, K.; Postma, R. S.; Bogaerts, A.; Lefferts, L. Plasma-Driven Catalysis: Green Ammonia Synthesis with Intermittent Electricity. *Green Chem.* **2020**, *22* (19), 6258−6287.
(48) Thirumdas, R.; Kothakota, A.; Annapure, U.; Siliveru, K.; Blundell, R.; Gatt, R.; Valdramidis, V. P. Plasma Activated Water (PAW): Chemistry, Physico-Chemical Properties, Applications in Food and Agriculture. *Trends Food Sci. Technol.* **2018**, *77*, 21−31.
(49) Dinh, D. K.; Muzammil, I.; Kang, W. S.; Kim, D.; Lee, D. H. Reducing Energy Cost of in Situ Nitrogen Fixation in Water Using an Arc-DBD Combination. *Plasma Sources Sci. Technol.* **2021**, *30* (5), 55020.

https://doi.org/10.1021/acsenergylett.1c01497
ACS Energy Lett. 2021, 6, 3004−3010